Analysis of Swing Characteristics for Floating Multi-Robot Towing System

Wei Chai, Zhigang Zhao, Dongna Li, Xiangtang Zhao, Ruina Chen, Jiadong Meng

Abstract—**The Floating Multi-Robot Towing System (FMRTS) tows a load on water using cables arranged in a parallel fashion. The presence of waves in the water can cause significant swinging of the load, which reduces the positioning accuracy and stability of the towing operation. Aiming at the uncertainty of load swing during the operation of FMRTS, the system's oscillation properties are examined utilizing ADAMS software. Firstly, the system's configuration is analyzed, and the dynamic model is developed using the Newton-Euler equations. Then, a 3D model of FMRTS is created, including the robot arm, load, and floating base. Based on this, the constraints and driving relationships of the system are configured to establish the system's virtual prototype. Finally, dynamic simulations of the system are conducted based on the virtual prototype. The load's oscillation characteristics are analyzed under the base's heave, roll, and heave-roll motions, determining the impact of the base's movements on the load's oscillations. The simulation results provide a reference for load anti-swing measures and lay the foundation for system stability analysis.**

Index Terms—**Multi-Robot Towing System, Load swinging, Dynamic simulation, Base motion, Virtual prototype**

I. Introduction

For towing operations in marine construction, bridge building, underwater salvage, and maritime rescue, there are high requirements for the load capacity and operational space of the towing equipment. Although traditional crane ships can meet these demands, they also have limitations. On one hand, large crane ships' development and maintenance costs are high, making it difficult to improve their utilization rate. On the other hand, the maritime surroundings are intricate and continuously shifting, especially due to natural factors such as wind and waves. These factors exert forces on the ship, causing severe swaying and exacerbating the swinging amplitude of the towed load, thereby presenting additional challenges and risks to the operations. In severe cases, it may even lead to the ship's capsizing.

In response to the inherent limitations of traditional crane ships in load capacity, operational scope, and positioning accuracy, a multi-robot towing system(MRTS) comprised of multiple floating crane robots is proposed. This system offers reconfigurability, substitutability, flexibility, and universality. Adjusting the relative positions of the floating crane robots, the positions of end-effectors, and the lengths of the cable can achieve changes in the pose of the towed objects, thereby achieving heavy-load towing operations.

Regarding classification, FMRTS can be categorized as cable-driven parallel robot systems(CDPR), but they differ significantly from traditional CDPR. CDPR involves fixing the position of one end of the cables to a specific moving mechanism, essentially functioning as a single robot. However, FMRTS are composed of modular and serially connected towing robots, making them inherently multi-robot systems. Currently, research on FMRTS is just beginning, but the achievements in CDPR can provide valuable insights for the study of FMRTS.

Research on the cable-driven multi-robot coordinated towing system has made some progress. F. Pierri [1] studied the cooperative transportation of unknown objects by aerial robots and designed two admittance filters to determine the trajectories of the load and the aerial robot, but did not consider the swinging of the load. N. Michael [2] discussed the static balance problem of the load in a multi-drone towing system under different pose states and analyzed the stability of the lifted object. Q. Jiang [3] developed the direct and reverse kinematic models for a multi-drone towing system and assessed the system's stability in static equilibrium using the Hessian matrix. Y. Ren [4] used the Lagrange equations to establish a rigid pendulum model for a helicopter towing system and proposed an energy-based control method to suppress load swinging. M. Bisgaard [5] utilized the Udwadia-Kalaba equation to establish a general model for single and multiple small-scale helicopter suspension transport systems and conducted simulation analysis. M. R. Mousavi [6] optimized the cable tensions for redundant constrained CDPR using a non-iterative analytical algorithm. E. A. Marchuk [7] explored the issue of positional and directional inaccuracies in the mobile platform of an extensive CDPR. It proposes a compensation strategy based on mathematical modelling and control algorithms. The strategy aims to mitigate the errors by considering the deformations of the cables and towers, thereby improving the robot's positioning accuracy and

Manuscript received April 3, 2024; revised November 6, 2024.

This work was supported by the National Natural Science Foundation of China (No. 51965032); the National Natural Science Foundation of Gansu Province of China (No. 22JR5RA319); the Science and Technology Foundation of Gansu Province of China (No. 21YF5WA060); and the Excellent Doctoral Student Foundation of Gansu Province of China (No. 23JRRA842).

Wei Chai is a PhD candidate of School of Lanzhou Jiaotong University, Lanzhou 730070, China. (e-mail: 403808465@qq.com).

Zhigang Zhao is a professor of School of Mechanical Engineering, Lanzhou Jiaotong University, Lanzhou 730070, China. (corresponding author to provide phone: 0931-4956047; fax: 0931-4938023; e-mail: zhaozhg@mail.lzjtu.cn).

Dongna Li is an associate professor of School of Mechanical Engineering, Lanzhou Jiaotong University, Lanzhou 730070, China. (e-mail: lidongna@mail.lzjtu.cn)

Xiangtang Zhao is a PhD candidate of School of Lanzhou Jiaotong University, Lanzhou 730070, China. (e-mail: 13220035@stu.lzjtu.edu.cn).

Ruina Chen is a graduate from Lanzhou Jiaotong University, Lanzhou 730070, China. (e-mail: 2212849028@qq.com).

Jiadong Meng is an associate professor of School of Mechanical Engineering, Lanzhou Jiaotong University, Lanzhou 730070, China. (e-mail: mengjiadong@foxmail.com).

motion precision. M. Carricato [8-10] pointed out that the kinematics and statics of CDPR are coupled. He proposed a geometric statics model for the system, introduced a novel geometric statics-solving method, and presented a point-to-point trajectory planning method. X. Zhao [11] investigated the stability of the wheeled mobile MRTS using an analysis method based on the stability cone technique. By establishing a system model and conducting stability evaluation, they determined the optimal joint angles of the robotic manipulation. D Li [12] focuses on analyzing the fluid-structure coupling effect in the towing system, discusses various factors that affect the system's stability, such as rope tension, the size and shape of the floating body, and external environmental factors. The steadiness of the floating robot is then evaluated using ship stability theory.

Research on marine towing systems has mostly focused on single crane ships, with few studies on FMRTS. T. V. Tao [13] studied the influence of floating cranes on static equilibrium during towing operations and proposed a method for calculating buoyancy and stability, focusing on the effect of changing the suspended load's position in relation to the inclination angle. M. M. Horoub [14] analyzed the workspace of a class of Stewart platforms under the influence of waves. C. Su [15-16] evaluated the stability of the FMRTS load by standardizing the minimum cable tension and the singular values of the stiffness matrix. H. Xu [17] utilized AQWA software to analyze the motion response characteristics of ore carriers in complex sea conditions, providing theoretical support for designing compensation systems for cargo holds. B. Li [18] studied the effects of cargo weight and rope length on the towing operation of a drilling vessel using a pendulum model and a point mass model. Additionally, the response characteristics under irregular waves were investigated through time-domain analysis.

Many researchers have studied multi-robot coordinated towing systems, but most have focused on cable tension, static stability, and path planning. Few studies specifically investigate the load swinging of multiple crane bases under the influence of waves. In this study, we established the spatial configuration and dynamic model of the FMRTS. A virtual prototype of the FMRTS, including the rope, was created using ADAMS software. Furthermore, we have conducted simulations to assess the dynamic properties of the system, focusing specifically on the swinging characteristics of the load under the effects of pitch, roll, and pitch-roll motions of the base.

II. System Configuration

The FMRTS is composed of three floating crane robots connected in parallel by cables. The system's spatial arrangement is depicted in Fig. 1. The floating crane robot is composed of a floating base and a folding arm crane. The floating base can be a waterborne engineering vessel with certain navigational capabilities or a floating work platform. The folding arm crane features three segments: the first link is attached to the floating base and is capable of rotating around the z-axis, while the second and third links rotate around their respective pivot points. Each folding arm crane has its end effector connected to the load via a cable. Manipulating the cranes' joint angles and cable lengths enables the load to be positioned in three-dimensional space. The global coordinate system, denoted as *O-XYZ*, serves as the fixed reference frame for the entire system, while the local coordinate systems, represented by *O`-X`Y`Z`* and O_i-$X_iY_iZ_i$ (for i=1, 2, 3), are attached to the load's center of mass and the bases of the cranes, respectively, providing relative positioning within the system.

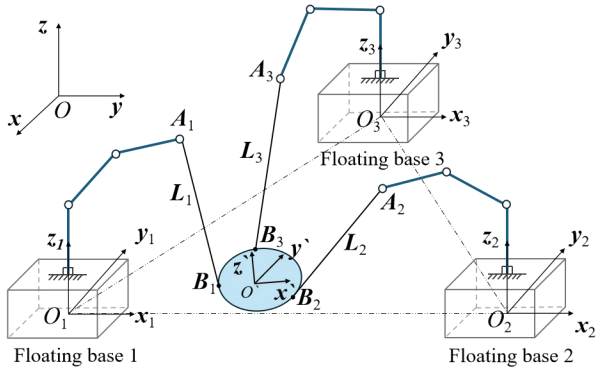

Fig. 1 Spatial configuration of the floating multi-robot towing system

Adjusting the position and orientation of the load can be achieved by changing the length of the cables and the position of the robot's end effector. Therefore, based on the different driving methods of the system, the system can be divided into three categories:

1) Fixed end effector position: Control the load's pose by adjusting the cables' length while keeping the end effector position fixed.

2) Constant cable length: The driving load is achieved by altering the end effector position without varying the cable length.

3) Simultaneous adjustment of cable length and end effector position: Regulate the load's pose by simultaneously modifying the cable lengths and the end effector's location.

III. Model of Floating Base Multi-Robot Towing System

Considering the complexity of the FMRTS structure, the following assumptions are made to simplify the system's dynamic model:

1) The floating crane robots are modelled as rigid bodies with uniform mass distribution. We neglect the influence of elastic deformation on the load's pose and do not consider the effect of the folding arm crane's rotation on the base pose.

2) The motion of the floating base under regular wave conditions is mainly characterized by heave and roll, following a sinusoidal motion pattern.

3) The mass and elastic distortion of the cables are disregarded, permitting the cables to swing around the crane's end effector position.

4) The connection of the cable to both the end effector of the crane robot and the load is assumed to be a frictionless ideal hinge.

A. Mathematical Model of Towing System

The mathematical model of the towing system can be established using the Newton-Euler equations. Based on Fig. 1, The cable's position vector, denoted as $\boldsymbol{L}_i$, can be formulated as:

$$\boldsymbol{L}_i = \boldsymbol{A}_i - \boldsymbol{r} - \boldsymbol{R}\boldsymbol{B}_i' \ (i = 1,2,3) \tag{1}$$

Where: $\boldsymbol{A}_i$ represents the position of the i-th crane's end effector in the global coordinate system O-XYZ, $\boldsymbol{r}(x, y, z)$ denotes the coordinates of the load's center of mass in the local coordinate system $O`$-$X`Y`Z`$, and $\boldsymbol{B}_i`$ signifies the position of the cable's attachment point to the load within the same local coordinate system.

The dynamic equations for the towing system are derived using the Newton-Euler formalism.

$$\begin{bmatrix} M\boldsymbol{I}_3 & \boldsymbol{0} \\ \boldsymbol{0} & \boldsymbol{I}' \end{bmatrix} \begin{bmatrix} \boldsymbol{a} \\ \dot{\boldsymbol{\omega}} \end{bmatrix} + \begin{bmatrix} \boldsymbol{0} \\ \boldsymbol{\omega} \times \boldsymbol{I}'\boldsymbol{\omega} \end{bmatrix} = \boldsymbol{A}^{\mathrm{T}} \boldsymbol{f} + \boldsymbol{G} \tag{2}$$

Where: M and $\boldsymbol{I}'$ respectively represent the mass and the inertia matrix of the load, $\boldsymbol{I}_3$ is the third-order identity matrix, $\boldsymbol{\omega} = [\dot{\alpha}\ \dot{\beta}\ \dot{\gamma}]^{\mathrm{T}}$ denotes the angular velocity of the load, and $\boldsymbol{a}$ and $\dot{\boldsymbol{\omega}}$ represent the linear and angular acceleration of the load, respectively.

Equation (2) depicts the cable tension as $\boldsymbol{f} = [f_1\ f_2\ f_3]^{\mathrm{T}}$, and the gravity matrix is denoted as $\boldsymbol{G} = -Mg[\boldsymbol{i}\ \boldsymbol{r} \times \boldsymbol{i}]^{\mathrm{T}}$, $\boldsymbol{i} = [0\ 0\ 1]^{\mathrm{T}}$, incorporating g for gravitational acceleration.The matrix $\boldsymbol{A}^{\mathrm{T}}$ is designated as the structural matrix:

$$\boldsymbol{A}^{\mathrm{T}} = \begin{bmatrix} \boldsymbol{u}_1 & \boldsymbol{u}_2 & \boldsymbol{u}_3 \\ \boldsymbol{B}_1 \times \boldsymbol{u}_1 & \boldsymbol{B}_2 \times \boldsymbol{u}_2 & \boldsymbol{B}_3 \times \boldsymbol{u}_3 \end{bmatrix} \tag{3}$$

Where: $\boldsymbol{u}_i$ is the unit vector of the cable:

$$\boldsymbol{u}_i = \frac{\boldsymbol{L}_i}{\|\boldsymbol{L}_i\|_2} = \begin{bmatrix} \frac{x_i - x}{L_i} & \frac{y_i - y}{L_i} & \frac{z_i - z}{L_i} \end{bmatrix}^{\mathrm{T}} \tag{4}$$

B. Virtual Prototype of the Towing System

A physical model is used to simulate and evaluate the performance and behavior of the FMRTS. The physical structure of the floating crane robot is modeled using SolidWorks software, as depicted in Fig. 2. In this model, non-essential elements like the base guardrail, which do not affect the simulation results are omitted during the modelling process. The folding arm crane consists of a slewing arm, pitch main arm, pitch sub-arm, and towing cable. The slewing arm is rigidly connected to the center of the base surface and can rotate around joint 1. The pitch main arm is connected to the slewing arm and can rotate around joint 2. The pitch sub-arm is connected to the end of the pitch main arm, and the towing cable is attached to the end of the pitch sub-arm. To prevent any motion interference, the model needs to undergo interference checks after assembly to ensure its correctness.

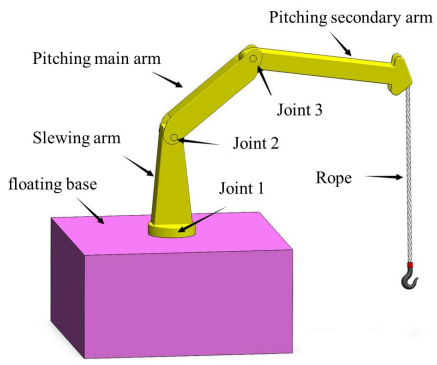

Fig. 2 Floating towing robot model

In SolidWorks, the three floating crane robots and the lifted object were assembled and arranged in the structural layout of the system's spatial configuration. The assembly was then exported as a Parasolid file format and imported into ADAMS software. The virtual prototype of the FMRTS created in ADAMS is shown in Fig. 3.

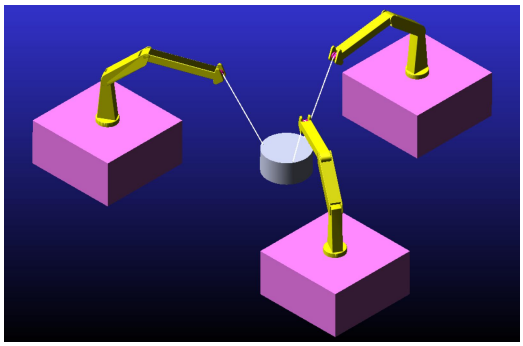

Fig. 3 Virtual prototype of a floating base multi-robot towing system

After importing the model created in SolidWorks into ADAMS, the original mates, material properties, and physical characteristics become invalid. It is necessary to redefine these relationships and properties in ADAMS. Additionally, forces, motion joints, and drives must be added to the model to enable simulation. Based on the actual actual operational circumstances of the floating base multi-robot towing system, drive functions should be added to the motion joints of the model in ADAMS. This allows the floating crane robot to follow the desired trajectory. The allocation of constraints is shown in Table I.

TABLE I
CONSTRAINTS ON SYSTEM COMPONENTS

Number	Connected Components	Constraint Type
1	Ground to Base	Universal Joint
2	Base to Slewing Arm	Rotational Joint
3	Slewing Arm to Pitching Main Arm	Rotational Joint
4	Pitching Main Arm to Pitching Secondary Arm	Rotational Joint
5	Cable to Load	Spherical Joint

C. Cable Model

The cable model created in SolidWorks is rigid and only has a connection relationship with the crane end and the load. Its length cannot be adjusted, which does not meet the system's towing conditions. In ADAMS 2018, the ADAMS/Cable module was introduced, which provides users with a convenient and efficient way to model cables and enables more accurate cable simulations. The module offers two methods for cable modelling: the simplified method and the discrete method.

The simplified method focuses on the synchronous motion between the steel cable and the pulley while neglecting the influence of cable vibration on the system. This method is based on the following assumptions: the steel cable remains in tension, there is no relative sliding between the cable and the pulley, and mass and friction are not considered. The advantage of this method is its simplicity in modelling and efficiency in simulation. It can effectively transmit forces and motion. However, it cannot accurately reflect the impact of vibration on the system and cannot simulate the winding behavior of the cable.

The discrete method divides the continuous cable into multiple rigid segments and uses constraints or axle forces to simulate the cable's flexibility. When the length of each segment relative to the entire cable is small enough, the cable's mechanical properties can be accurately simulated. The advantage of this method is its high degree of suitability to the actual situation, as it can simulate the winding action between the cable and the pulley. The drawback is that the model scale is larger, simulation results are sensitive to parameters, which may lead to simulation failures, and simulation speed is slower. Therefore, this method is suitable when considering cable weight and inertia parameters.

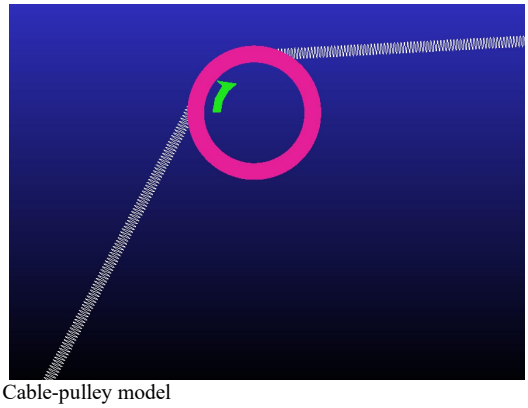

Fig. 4 Cable-pulley model

Based on the assumptions in this article, the simplified method is used for cable modelling. One cable end is connected to the load, and the other is connected to the pitch sub-arm. The extension and retraction are achieved through the pulley. The cable-pulley model is shown in Fig. 4, and its parameters are shown in Table II and Table III.

TABLE II
CABLE PARAMETERS

Diameter (mm)	Density (kg/m^3)	Preload (kg)	Young's Modulus	Damping Coefficient
25	1000	6250	1.0E11	0.01

TABLE III
PULLEY PARAMETERS

			Cable-Pulley Contact Parameters		
Diameter (m)	Width (m)	Density (kg/m^3)	Friction Coefficient	Contact Stiffness (N/m)	Approach Contact Velocity (m/s)
0.3	0.2	7801	0.6	1.0E8	0.1

IV. Simulation of Motion Performance of Towing System

Referring to the theory of ship motion on waves, the base's movement under regular wave action is primarily characterized by heave and roll, exhibiting motion patterns akin to sinusoidal behavior. In the present study, sea state 3 is selected as the external excitation for the system, with the relevant frequency and wave height are determined based on the data from the reference [19]. The base is designed as a rectangular platform with dimensions of 4 m (length) × 4 m (width) × 2 m (height). Undersea state 3, the base experiences heave motion along the Z-axis with the following wave characteristics: a wave direction of 0°, an effective wave height of 0.5 m, a wave amplitude of 0.4 m, and a frequency of 0.785 rad/s. Additionally, the base also experiences roll motion around the X-axis with an amplitude of 2° and a frequency of 1.05 rad/s. Notably, Due to wave action, there is a phase difference of 90° between roll and heave motion.

The mass of the load is 2.45×10^4 kg, and its initial center of mass pose is (0 m, 0 m, 0.5 m, 0, 0, 0). The target position for towing is (1.25 m, 0 m, −0.5 m, 0, 0, 0), which requires the load's orientation to remain unchanged during towing. Assuming the load first descends 1 m in the Z-direction and then translates 1.25 m in the X-direction. The system's driving process is structured as follows:

Stage 1 (0-50 s): The joints of the crane robots remain fixed, and the three cables extend at the same rate to achieve the vertical descent of the load.

Stage 2 (50-100 s): The cable lengths are fixed. The joint 1 of crane robots 1 and 2 rotate around the Z-axis to achieve the horizontal translation of the load. The joint 3 of crane robot 3 rotates around the Y-axis to coordinate with robots 1 and 2, ensuring that the load's orientation remains unchanged.

Stage 3 (100-150 s): The crane robot's joint angles and cable lengths are held constant. The entire towing process occurs in sea state 3, during which the base undergoes only heave motion.

In ADAMS, the heave motion of the base can be set as a sinusoidal driving function. The joint velocities of the crane robot and the cable velocities can be approximated using a third-orde polynomial representation of the step function, expressed as step(*time*, t_0, x_0, t_1, x_1), where *time* is the time variable, t_0 is the initial time, x_0 is the initial function value, t_1 is the termination time, and x_1 is the function termination value. The duration of the simulation is set at 150 seconds, using a time step of 0.1 seconds. The analysis focuses on the load's pose and cable tension during the towing process. The simulation process is shown in Fig. 5.

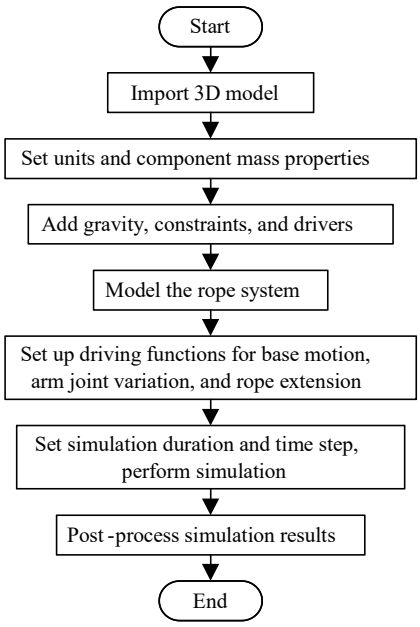

Fig. 5 Simulation flow in ADAMS

The movement of the load's center of mass throughout the

towing operation is depicted in Fig. 6. Owing to the base's upward and downward motion, the displacement in the Z-direction exhibits a sinusoidal pattern. From 0 to 50 s, there is an overall downward trend. Between 50 and 75 s, the load fluctuates around $z = -0.6$ m. From 75 to 100 s, there is a slight upward movement. At 100 s, the load reaches the $z = -0.5$ m position. Between 100 and 150 s, the load follows the motion of the base and undergoes sinusoidal oscillation around $z = -0.5$ m. In the X-direction, the load change is not displaced from 0 to 50 s. The displacement gradually increases from 50 to 100 s, reaching a final value of $x = 1.25$ m at 100 s, and remains constant thereafter. In the Y-direction, the displacement of the load does not change throughout the towing process. The results indicate that the parameters set for the virtual prototype can meet the driving objectives and achieve the desired changes in the load's position.

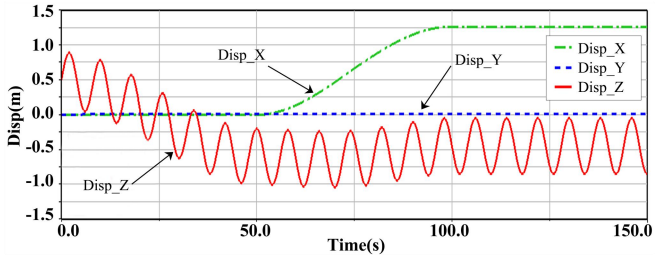

Fig. 6 Displacement variation curve of load

The orientation angles of the load during the towing process are shown in Fig. 7. At the moment of towing, there is a sudden change in the load's orientation angles, which is caused by the inertia of the cables. From 0 to 50 s, the orientation angle around the X-axis fluctuates around 0.5°. The orientation angle around the Y-axis fluctuates around 1°, and after 50 s, it decreases and then increases again. After 100 s, it stabilizes at −0.5°. The orientation angle around the Z-axis remains nearly constant throughout the simulation. At the end of the simulation, the load's orientation angles are (1°, −0.5°, 0°).

Due to FMRTS being an under-constrained system, it cannot precisely control the displacement and orientation of the load, which may result in swinging during the towing process. Simulation results show that the load's orientation angle variation is minimal and close to the target direction. This indicates that the virtual prototype can meet the requirements for maintaining a stable orientation angle during towing.

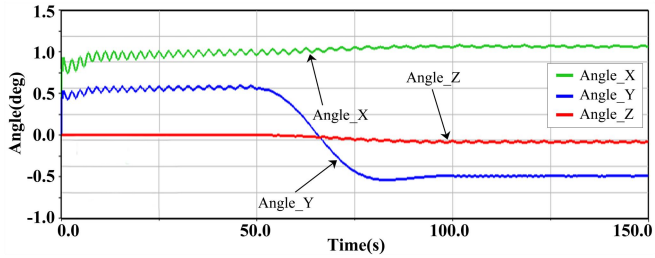

Fig. 7 Attitude angle variation graph of loads

The cable tensions during the towing process are shown in Fig. 8. From 0 to 50 s, all three cables extend at the same rate, with the tension changes uniformly. From 50 to 100 s, as the end positions of the crane robots, the tensions of cables 1 and 2 gradually increase, whereas the tension of cable 3 gradually decreases. This is due to the inconsistent motion of the joint mechanisms between robot 3 and robots 1 and 2. After 100 s, when the load reaches the target position, the tensions of all three cables exhibit minor harmonic variations. As a result, the cable tensions exhibit small harmonic variations near an equilibrium position, resembling wave-like oscillations. The cable tensions follow the movement of the floating base and gradually enter a self-balancing state owing to their restorative capabilities.

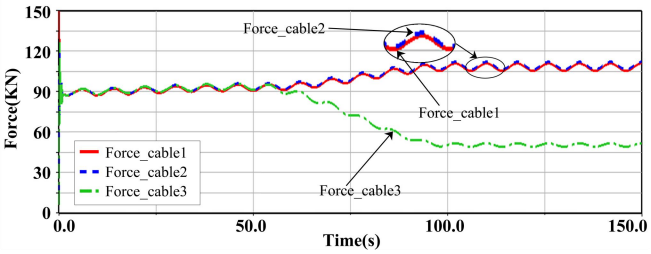

Fig. 8 Variation curve of cable tension

The torque variations of the joints for each of the three floating robots are measured. The torque variations of Joint 1 for each robot are shown in Fig. 9, and the torque variations of Joint 3 for each robot are shown in Fig. 10. Here, $Joint_{ij}$ represents the j-th joint of the i-th floating robot. It can be observed that the driving method of the system directly impacts the torque experienced by the joints of the floating robots, and the torque variations align closely with the trends in cable tensions.

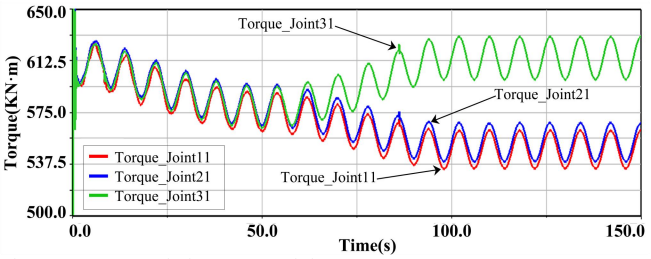

Fig. 9 Moment variation curve at joint 1

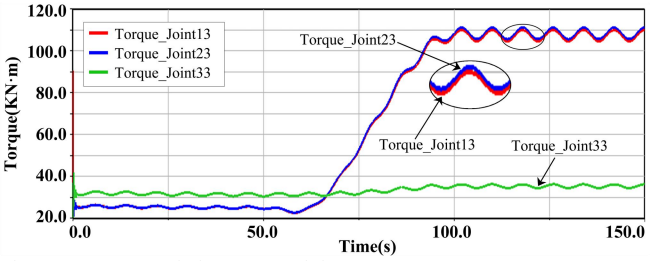

Fig. 10 Moment variation curve at joint 3

V. Effect of Base Motion on Load Rocking

The FMRTS is affected by sea wave and wind load during the towing process, causing the system's base and load to swing. The swing of the load reduces the positioning accuracy and stability of the towing operation. To gain a deeper understanding of the impact of base sway on load swing within the FMRTS, this study explores the characteristics of load swing in response to base sway. The simulations are conducted under sea condition parameters of sea state 3, and the simulation duration is set to 100 s with a time step of 0.1 s.

In order to provide a comparative analysis, the simulation is first conducted without wave excitation, representing the scenario when the system is on an ideal calm water surface. The simulation results are shown in Fig. 11. The data reveal that during the initial 10 s, the pose of the load exhibits minor fluctuations that gradually diminish. After 10 s, the pose of the load tends to stabilize. This occurrence is due to the model's uneven mass distribution and the cables' inertial effects.

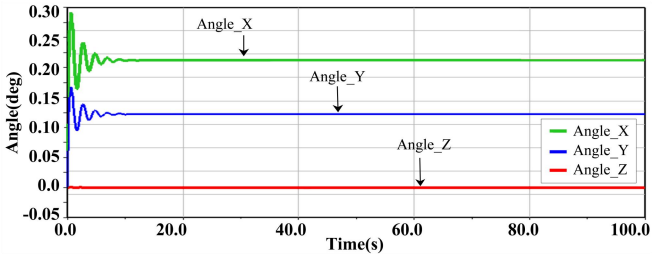

Fig. 11 Load pose with no wave excitation

The FMRTS is an underconstrained system, and the complex towing environment can cause the base to sway, which in turn reduces the stability during the towing process. To study the load's swing characteristics under the base's sway, the base is set as heave motion, roll motion, and heave-roll motion in the simulation environment.

A. Heave Motion of the Base

When the base undergoes only heave motion, the swing of the load is shown in Fig. 12(a)-(c). The load's movement in the X, Y, and Z axes fluctuates periodically with time. The displacement fluctuations in the X and Y directions are relatively small, with the amplitude of these fluctuations decreasing gradually with time. However, the displacement in the Z direction is related to the driving function of the base heave motion, with an amplitude of 0.4 m. The swing amplitude of the load around the X-axis is approximately 0.2°, around the Y-axis is approximately 0.15°, and almost no swing around the Z-axis. This suggests that the load's orientation angles exhibit only minor variations, particularly in the Z-axis rotation when no external driving forces are acting upon it.

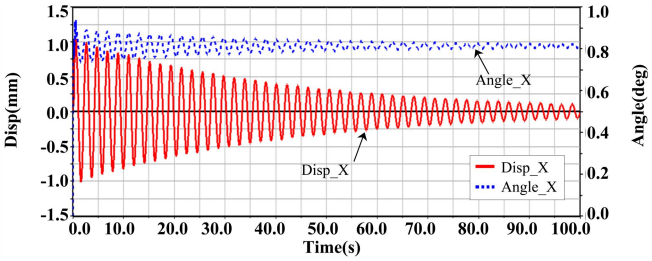

(a) Pose of the load in the X direction

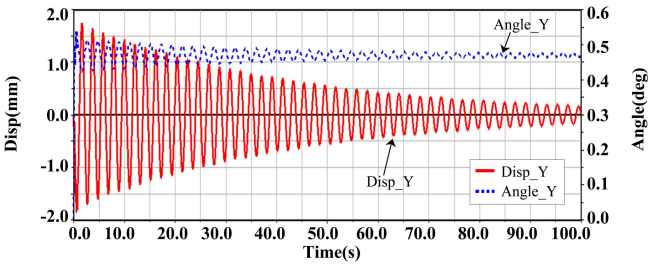

(b) Pose of the load in the Y direction

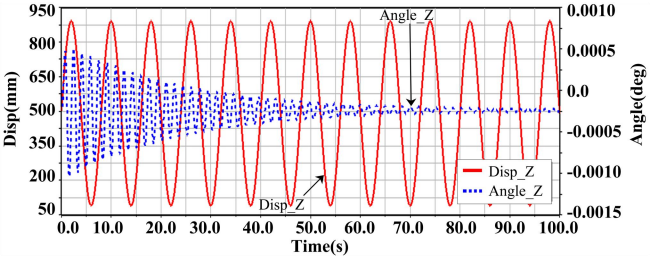

(c) Pose of the load in the Z direction

Fig. 12 Load pose during base pendulum motion

B. Roll Motion of the Base

When the base undergoes only roll motion, the swing of the load is shown in Fig. 13(a)-(c). The movement of the load in the X direction varies within the range of −0.4 m to 0.4 m, with a relatively stable amplitude. The oscillation angle around the X-axis gradually increases over time, eventually reaching an oscillation angle between −0.5° to 2°. On the contrary, the movement of the load in the Y direction increases gradually over time, with the maximum displacement ranging from −0.03 m to 0.025 m, and overall small fluctuations. The swing around the Y-axis has a periodic nature with a relatively stable amplitude, ranging from −10° to 10°. The displacement of the load in the Z direction varies within the range of 0.49 m to 0.505 m, also exhibiting small fluctuations. The swing angle around the Z-axis gradually increases from 0° to 4°.

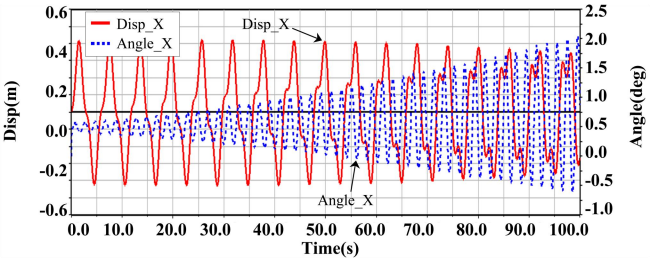

(a) Pose of the load in the X direction

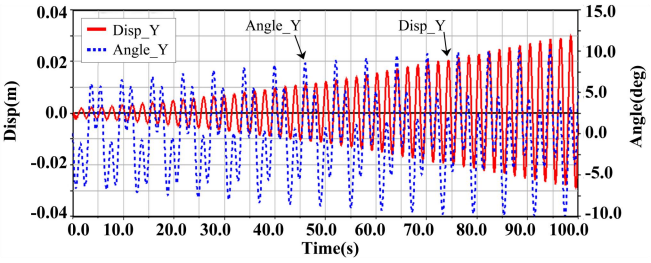

(b) Pose of the load in the Y direction

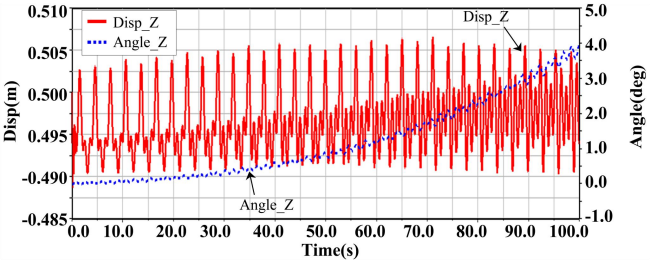

(c) Pose of the load in the Z direction

Fig. 13 Load pose during the base transverse swing motion

C. Heave-roll Motion of Base

When the base undergoes both heave and roll motion simultaneously, the swing of the load is depicted in Fig.

14(a)-(c). The displacement of the load in the X direction varies within the range of −0.7 m to 0.7 m, and the swing angle around the X-axis ranges from −20° to 20°. In the Y direction, the displacement of the load varies within the range of −0.55 m to 0.55 m, and the swing angle around the Y-axis ranges from − 15° to 15°. In the Z direction, the displacement of the load varies within the range of −0.425 m to 0.725 m. The swing around the Z-axis does not exhibit a regular pattern, and the peak swing angle is 12°.

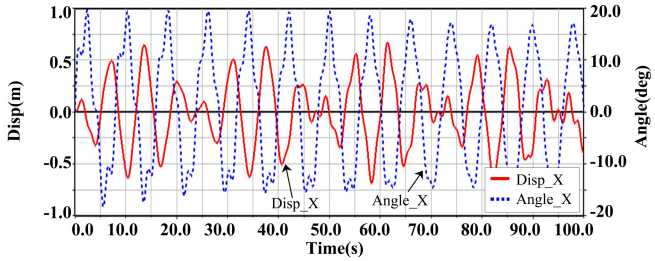

(a) Pose of the load in the X direction

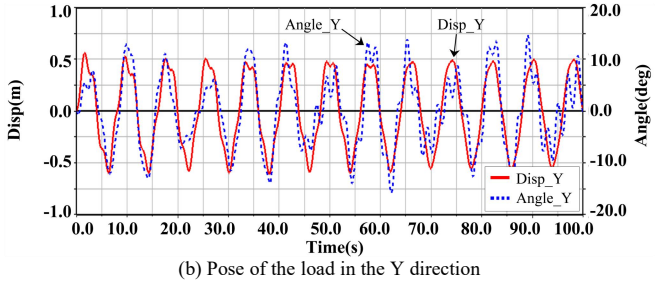

(b) Pose of the load in the Y direction

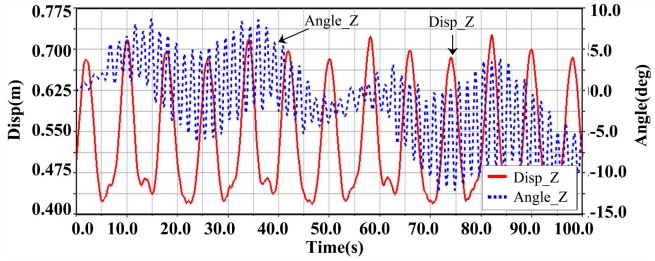

(c) Pose of the load in the Z direction

Fig. 14 Pose of the load under base heave-roll motion

In summary, It is noticeable that the vertical movement of the base exerts the least influence on the load sway, mainly impacting the displacement along the Z direction. In contrast, the roll motion of the base significantly affects the displacement in the X direction and the swing around the Y-axis. When both heave and roll motions are combined, the load experiences significant fluctuations in displacement and swing amplitudes in all directions. If the swing amplitudes exceed the allowable safety range for towing operations, effective measures must be taken to mitigate the swing. Failure to do so can compromise the safety and stability of the towing operation.

VI. Conclusion

This research employed the Newton-Euler approach to dissect the kinematic and dynamic equations of the FMRTS. The kinematic and dynamic simulations were conducted using ADAMS, and load position and pose changes under the action of the base swing were obtained. Based on the analysis of the experimental data, the following conclusions can be made:

1) The motion performance was conducted for the towing system. The changes in the load's pose and the tension in the cables have been discussed and analyzed using different driving methods and base heave. The results indicated that, due to the underconstrained nature of the FMRTS, the load exhibited minor oscillations, with the main cause being the base oscillations.

2) The swing behavior of the load under the effects of base heave, roll, and heave-roll motions was analyzed. The results demonstrated that when both heave and roll motions acted on the base, the load exhibited significant displacement and swing amplitude fluctuations in all directions. Effective measures should be taken to reduce swing and prevent oscillations to ensure operational safety and system stability.

The simulation results provided references for swing reduction and oscillation prevention of the load, laying a foundation for system stability analysis.

References

[1] F. Pierri, M. Nigro, G. Muscio, and F. Caccavale, "Cooperative Manipulation of an Unknown Object via Omnidirectional Unmanned Aerial Vehicles," *Journal of Intelligent & Robotic Systems*, vol. 100, no. 3, pp. 1635-1649, 2020.

[2] N. Michael, J. Fink, and V. Kumar, "Cooperative manipulation and transportation with aerial robots," *Autonomous Robots*, vol. 30, no. 1, pp. 73-86, 2011.

[3] Q. Jiang and V. Kumar, "Determination and Stability Analysis of Equilibrium Configurations of Objects Suspended From Multiple Aerial Robots," *Journal of Mechanisms and Robotics*, vol. 4, no. 2, 2012.

[4] Y. Ren, K. Li, and H. Ye, "Modeling and anti-swing control for a helicopter slung-load system," *Applied Mathematics and Computation*, vol. 372, p. 124990, 2020.

[5] M. Bisgaard, J. D. Bendtsen, and A. l. Cour-Harbo, "Modeling of Generic Slung Load System," *Journal of Guidance Control and Dynamics*, vol. 32, pp. 573-585, 2009.

[6] M. R. Mousavi, M. Ghanbari, S. A. A. Moosavian, and P. Zarafshan, "Rapid and safe wire tension distribution scheme for redundant cable-driven parallel manipulators," *Robotica*, vol. 40, no. 7, pp. 2395-2408, 2022.

[7] E. A. Marchuk, Y. V. Kalinin, and A. Maloletov, "Error Compensation in Position and Orientation of Mobile Platform of Cable-Driven Robots via Tensile Forces Measurement," *Mekhatronika, Avtomatizatsiya, Upravlenie*, vol. 23, pp. 515 - 522, 2022.

[8] G. Abbasnejad and M. Carricato, "Direct Geometrico-static Problem of Underconstrained Cable-Driven Parallel Robots With n Cables," *IEEE Transactions on Robotics*, vol. 31, no. 2, pp. 468-478, 2015.

[9] M. Carricato, G. Abbasnejad, and D. Walter, "Inverse Geometrico-Static Analysis of Under-Constrained Cable-Driven Parallel Robots with Four Cables," *Advances in Robot Kinematics*, 2012.

[10] E. Idà, T. Bruckmann, and M. Carricato, "Rest-to-Rest Trajectory Planning for Underactuated Cable-Driven Parallel Robots," *IEEE Transactions on Robotics*, vol. 35, no. 6, pp. 1338-1351, 2019.

[11] X. Zhao, Z. Zhao, S. Zhang, and C. Su, "Stability analysis of wheeled mobile multi-robot coordinated towing system," *Journal of Mechanical Science and Technology*, vol. 36, no. 1, pp. 407-416, 2022.

[12] D. Li, X. Zhao, Z. Zhao, C. Su, and J. Meng, "Stability Analysis of the Floating Multi-robot Coordinated Towing System Based on Ship Stability," *Engineering Letters*, vol. 32, no. 6, pp. 1191-1200, 2024.

[13] T. V. Tao and N. C. Luy, "The Effect of the Change in the Position of Load on the Inclination Angle of Floating Crane," *International Journal of Transportation Engineering and Technology*, 2020.

[14] M. M. Horoub, M. Hassan, and M. A. Hawwa, "Workspace analysis of a Gough-Stewart type cable marine platform subjected to harmonic water waves," *Mechanism and Machine Theory*, vol. 120, pp. 314-325, 2018.

[15] C. Su, J. Li, W. Ding, and Z. Zhao, "Static workspace analysis of a multi-robot collaborative towing system with floating base," *International Journal of Modeling, Simulation, and Scientific*

Computing, vol. 12, pp. 2150009, 2021.
[16] C. Su, X. Zhao, Z. Yan, Z. Zhao, and J. Meng, "Load Stability Analysis of a Floating Multi-Robot Coordinated Towing System," *Journal of Shanghai Jiaotong University*, 2023.
[17] H. Xu, P. Neng, and F.-q. Yang, "Motion response analysis of mining vessel based on ANSYS/AQWA," *Journal of Physics: Conference Series*, vol. 1300, 2019.
[18] B. Li, W. Huang, and X. Chen, "A numerical study of dynamic response of crane semi-submersible along TLP in tender-assisted drilling operation," *Ships and Offshore Structures*, vol. 13, pp. 273 - 286, 2018.
[19] J. V. Heiden, "Vessel and cargo motions: A frequency domain method to study combined vessel and cargo responses," *Engineering, Physics* 2019.

Wei Chai, born in 1995, is a PhD candidate of Lanzhou Jiaotong University. His primary research focus lies in the field of multi-robot systems modeling and control.